

Elucidation of the thickness inside the niobium anodic oxide film and its effect on adhesion to polyimide film

Munenori Yoshida^{a,*}, Hiromi Yamanaka^b, Kenta Tomori^c, Sergei A. Kulinich^{c,d}, Syuuichi Maeda^{b,c,e}, Satoru Iwamori^{a,b,c,d}

^a Graduate School of Science and Technology, Tokai University, 4-1-1 Kitakaname, Hiratsuka-shi, Kanagawa, 259-1292, Japan

^b Graduate School of Engineering Tokai University, 4-1-1 Kitakaname, Hiratsuka-shi, Kanagawa, 259-1292, Japan

^c Department of Mechanical Engineering Faculty of Engineering, Tokai University, 4-1-1 Kitakaname, Hiratsuka-shi, Kanagawa, 259-1292, Japan

^d Research Institute of Science and Technology, Tokai University, 4-1-1 Kitakaname, Hiratsuka-shi, Kanagawa, 259-1292, Japan

^e Department of Optical and Image Engineering, Tokai University, 4-1-1 Kitakaname, Hiratsuka-shi, Kanagawa, 259-1292, Japan

ARTICLE INFO

Keywords:

Anodizing
Niobium
Plasma treatment
Reflectance
Flexible material
Adhesion strength

ABSTRACT

Niobium oxide films prepared via anodic oxidation are known to exhibit various colors. These colors are affected by the voltage during anodizing treatment to produce such thick film. The anodic oxidation reaction stops when the applied voltage reaches its saturation value. At this point the film stops growing, its thickness of the internal oxide layer being proportional to the applied voltage. Therefore, this study aims to clarify the relationship between the oxidation state inside the anodized film and its thickness.

We also attempted to anodize a polyimide (PI) film, which is a flexible resin material. Because such a PI film is nonconductive, it was sputter-coated with an intermediate layer of niobium before anodization. To enable adhesion to the PI film, the Nb-sputtered film was subjected to surface modification via oxygen plasma treatment. Finally, the Nb-coated PI film was subjected to anodization. Detailed optical comparison was performed between the anodized Nb-coated PI substrate and anodized Nb plate substrate.

1. Introduction

Oxide films of metals such as titanium, cobalt, zirconium, tantalum, and niobium (Nb) exhibit various colors related to interference phenomena [1–11]. Niobium oxide (Nb₂O₅) films have been prepared via various chemical and physical approaches [12–17]. A simple technique for fabricating Nb₂O₅ is anodization, in which a stable oxide layer is formed on the surface. This method also aids resistance to corrosion and abrasion and enables uniform processing over a large area at low costs [18]. Anodization converts Nb into Nb₂O₅, a highly refractive material that exhibits chemical and thermal stability and vivid coloration. The thickness of such a film is typically on the order of visible-light wavelengths and determines its color. Coloring by means of structures with dimensions of visible-light wavelengths or finer, also known as “structural color”, differs from coloring by pigments. Structural color is particularly energy efficient because it achieves color without losing light energy. Moreover, unlike dye coloring, it is not discolored by ultraviolet rays. Nb₂O₅ is a highly refractive material (refractive index = 2.45) that shows vivid colors and exhibits excellent chemical and

thermal stability. Therefore, Nb₂O₅ has prospects in future decorative applications [19]. Films formed on Nb are expected to realize Nb₂O₅ film materials with a high refractive index.

Previous studies demonstrated that the thickness of Nb₂O₅ layer prepared via anodization depends on applied voltage. Further, the anodization process stops automatically, producing film thickness that is proportional to the applied voltage. Komatsu et al. reported that the color shade of anodized Nb films was related to the thickness of produced Nb₂O₅ layers [20].

However, the chemical state of the film providing the color shade has not yet been analyzed.

Therefore, we examined the internal structure of the thin film and analyzed the relation between the chemical state of the thin film and its color.

Recently, technologies delivering ultrathin and miniaturized electronic devices have advanced remarkably. Polymer materials are often preferable owing to their low weight and high flexibility [21]. Polyimide (PI) films are particularly used as flexible substrates and parts of electronic equipment because of their flexibility, heat resistance, chemical

* Corresponding author.

E-mail address: 7ltad007@mail.u-tokai.ac.jp (M. Yoshida).

<https://doi.org/10.1016/j.vacuum.2021.110265>

Received 27 September 2020; Received in revised form 14 April 2021; Accepted 15 April 2021

Available online 1 May 2021

0042-207X/© 2021 Elsevier Ltd. All rights reserved.

resistance, and low coefficient of linear expansion [22–24]. However, PI films are hydrophobic and possess low adhesion to metals [18,24–26]. To address this problem, the surfaces of metal materials are oxidized, typically via anodic oxidation, which easily forms an oxide layer on their surface. However, fabricating a curved-colored workpiece from Nb is difficult because Nb, similar to Ta and Mo, is a material that is difficult to cut. Therefore, to prepare a thin Nb film with high adhesion on a flexible material, normally sputtering method is used followed by an anodizing treatment. Initially, we considered Nb₂O₅ films with high adhesion to a flexible material (PI) fabricated using this approach.

However, Nb films deposited on non-modified PI substrates tend to peel off, which is why oxygen plasma treatment was chosen as a conventional surface modification approach. Plasma etching increases the surface roughness and provides hydrophilic functional groups that improve adhesion to as-processed surface [27–29].

In the present study, we established oxygen plasma treatment conditions that ensure a good adhesion of sputtered Nb films to PI substrate and guarantee a high adhesion strength. Additionally, after anodizing, the adhesiveness of the Nb₂O₅ films was mechanically and optically evaluated. This way, excellent coloring properties of Nb₂O₅ were easily imparted to materials that are difficult to dye or paint. Furthermore, the effect of the internal structure of anodic Nb₂O₅ film on its color was carefully investigated. Among other goals, this study aimed to develop a methodology to accomplish this task, with Fig. 1 showing the structure of a studied sample.

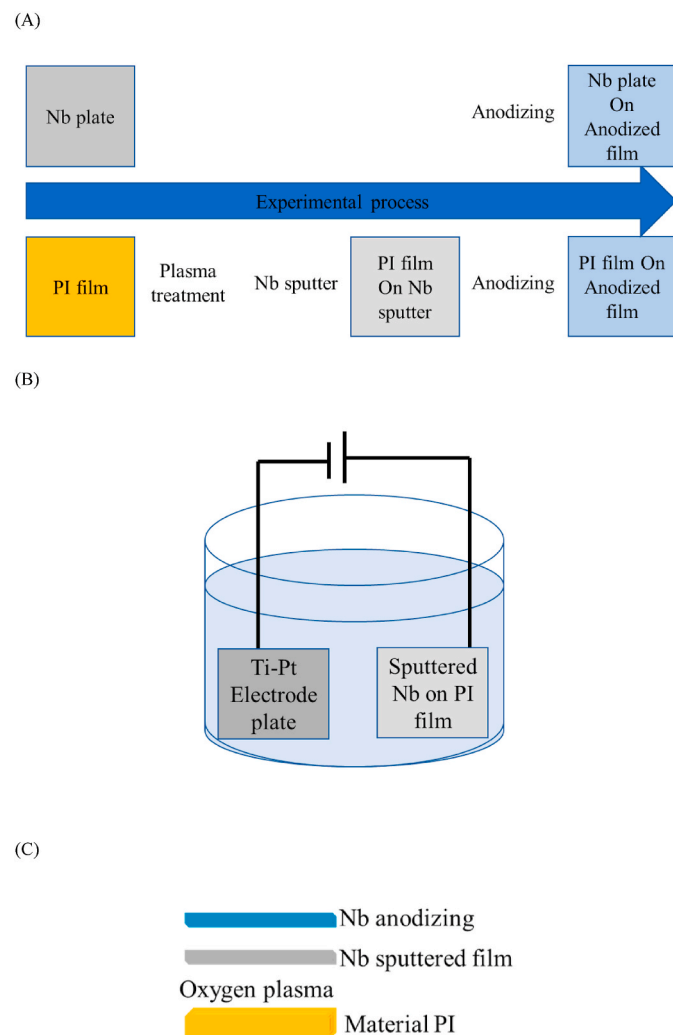


Fig. 1. (A) Experimental process; (B) Anodizing; (C) Schematic of film layers.

2. Experimental method

2.1. Anodizing conditions

Metal Nb films were sputter-deposited on PI films at the anode side of a DC power supply. Platinum (Pt) was connected to the cathode side as electrode. The structure was immersed in 5% citric acid prepared in pure water and subjected to voltages of 20, 60, or 100 V for 5 min. Under the voltage application, an oxide film (thickness of approximately 50–250 nm) was formed on the metallic Nb film. For comparison, a metal Nb substrate was also subjected to anodic oxidation treatment. The anodizing conditions are presented in Table 1. The anodized Nb films formed on the PI film and metal Nb are referred to as samples on PI substrate and samples on Nb substrate, respectively. XRD and XPS were used to analyze the inside of as-prepared anodized films. Upon anodizing treatment, the sample surface was studied using XRD (XRD-D8, DISCOVER Bruker) to determine the surface and internal conditions of the anodized film. After oxygen plasma treatment, the PI substrate surface was analyzed using XPS (PHI Quantera II; ULVAC-PHI). Because some points must be considered when performing XPS analysis [30–33], the following conditions were established to conduct the analysis. The pressure in the chamber was confirmed to be 1.4×10^{-6} Pa or more, and Al K α was used as X-ray source at an angle of 45°. Further, C 1s and O 1s XPS spectra of the PI surface were obtained under the condition of 1.00-V Neutralizer Energy with 20- μ A charge neutralizer Current. Photoelectron spectroscopy software (PHI Multi PakTM Version9, ULVAC-PHI Inc.) was used for spectrum analysis. The size of prepared samples was ~ 6 mm.

Surfaces were also analyzed after testing the adhesion strength of Nb₂O₅ layer formed on both PI and anodized Nb substrates. Furthermore, the state of the anodized Nb substrate was analyzed.

2.2. Surface modification conditions

The PI film (Kapton® 200H, thickness 0.05 mm, manufactured by Toray DuPont) was cut into dimensions of 50 mm \times 40 mm and sonicated with ethanol (99.5%, Wako Pure Chemical Industries). After cleaning for 5 min, the film was sputter-coated with Nb, then treated with oxygen plasma and anodized at different voltages and for different times. As a result, optimal anodizing conditions were determined in a comparative study. The oxygen plasma treatment was applied using a plasma device (RFS-200 from ULVAC). Previously, we reported on the effect of etching [34], and the presence of CO⁺ and CO₂⁺ was confirmed when etching was high. In this study, the pressure was reduced during surface modification. Fig. 1(A)–(C) show the experimental procedures and film layers. Experimental conditions for oxygen plasma treatment are provided in Table 2. Subsequently, a 500-nm Nb-sputtered film was fabricated.

2.3. Evaluation of wettability

Wettability measurements confirmed the surface modification effect on PI substrates after their treatment with oxygen plasma. The wettability was evaluated using a contact angle goniometer (LSE-ME3). For such measurements, 5 μ L of pure water was dropped from a height of 10 mm above the sample and the contact angle of the drop was photographed. Next, diameter d and height h of the photographed water

Table 1
Anodizing conditions.

Anode	Nb
Cathode	Pt
Electrolytic solution	Citric acid aqueous solution (5%)
Voltage (V)	10–100
Deposition time (min.)	5

Table 2
Experimental conditions of oxygen plasma treatment.

Oxygen plasma		Niobium sputtering	
Inflow gas	O ₂	Inflow gas	Ar
Gas flow (ccm)	4	Gas flow (ccm)	100
Operating pressure (Pa)	3.5	Operating pressure (Pa)	1.6
Back pressure (Pa)	2.0×10^{-2}	Back pressure (Pa)	8.0×10^{-5}
RF Power (W)	25, 50, 100	RF Power (W)	100
Deposition time (min.)	1,3,5	Thickness (nm)	100

droplet were analyzed, and the contact angle was measured using the $\theta/2$ method (see formula (1) below). The results were reported as the average of five measurements.

$$\theta = 2 / \tan(2 h/d) \quad (1)$$

2.4. Adhesion strength test

Anodization was performed after surface modification of the PI film followed by sputter-deposition of metallic Nb layer. The adhesive strength between the Nb₂O₅ film and its PI substrate was measured using a tensile tester (SV-55C-2M, LV-200 N; Imada Seisakusho). The adhesive used for the tensile tester was araldite rapid-curing-type adhesive. The adhesive force was measured at a drying temperature of 40 °C and a feed speed of 10 mm/min for 14 h. Fig. 2 presents schematically both the apparatus and the sample, while formula (2) was used to evaluate the adhesion force:

$$\text{Adhesive force (Pa)} = \text{load (N)}/\text{specimen area (m}^2\text{)} \quad (2)$$

The following formula was used for adhesion:

$$\text{Adhesive force (Pa)} = \text{load (N)}/\text{specimen area (m}^2\text{)}.$$

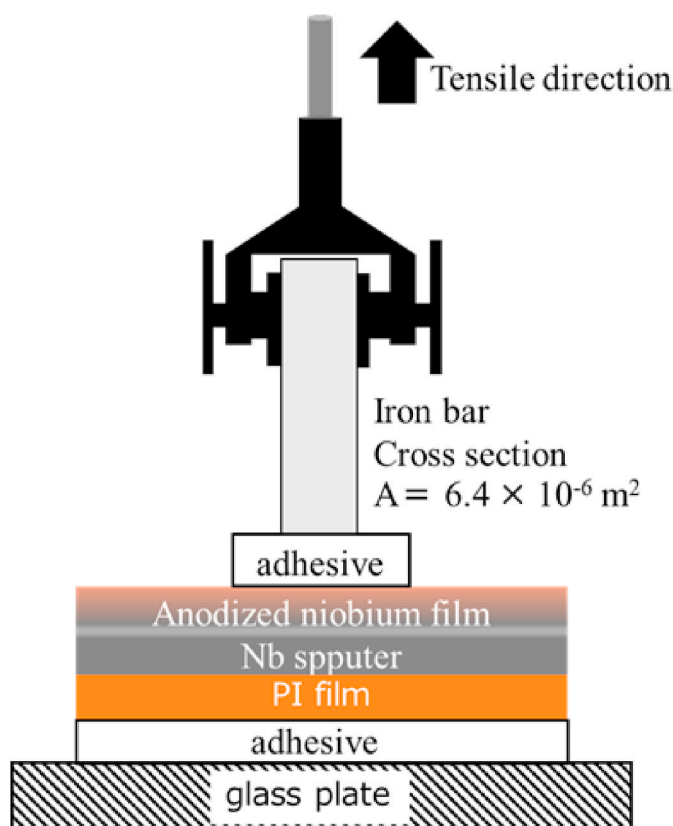


Fig. 2. Schematic of the adhesion test.

2.5. Reflectance measurements using a spectrophotometer

The reflectance of samples on both PI and Nb substrates was measured using a spectrophotometer (V-670; JASCO Corporation), after which their spectra were compared. The measurement conditions were as follows: visible light range of 250–800 nm and stepping of 1°. The incidence angle was set using a 5° S wave.

3. Results and discussion

3.1. Anodized films

Fig. 3 shows optical images of anodized Nb films prepared at different voltage applied to the Nb plate substrate. This observation is well consistent with our previous work and confirm good reproducibility of results of the present experiments [19].

XRD gives information on phase composition and can analyze samples much deeper inside the films. The XRD pattern of a sample prepared via anodizing Nb substrate at 100 V is shown in Fig. 4. It is clearly seen that a mixed layer of NbO and Nb₂O₅ was formed inside the film, while no obvious signals of NbO₂ are seen in the XRD pattern. Therefore, we conclude that the surface is mainly based on Nb₂O₅, whereas the inside is a mixed layer of NbO and Nb₂O₅.

To determine the internal state of anodized films, Figs. 5 and 6 exhibit the XPS spectra of a sample prepared via anodization at 100 V. Spectra in Fig. 5 demonstrate Nb3d peaks whereas Fig. 6 presents O 1s peaks. Lines with different colors show spectra measured on untreated surface (blue) and then after 0.1, 0.2, 0.3 and 53.0 min of surface sputter etching. It is already reported that analyzing the C 1s peak of accidental carbon is a dangerous procedure [30–33]. Generally, adventitious carbon is an unknown compound, which is not an inherent part of the sample, and it does not make proper electrical contact to the analyzed sample; moreover, BE of the C 1s peak varies in a wide range. Therefore, the analyzed data are shown in Figs. 5 and 6 without any adjustment. From the XPS results, the outermost surface was Nb₂O₅, and from the XRD results, the internal compounds were identified Nb₂O₅ and NbO mixtures. However, there can be observed thin layers different from the Nb₂O₅ and NbO at the 0.1 min of surface sputter etching. As the NbO₂ cannot be observed from the XRD spectrum shown in Fig. 4, it is considered that there is very thin or no NbO₂ layer between the Nb₂O₅ and Nb₂O₅–NbO mixture layers [35,36].

Next, the difference in colors was considered by performing anodic oxidation treatment. Figs. 7 and 8 show the elemental ratios of Nb₂O₅, NbO, and Nb in the anodized layer produced at voltages of 60 and 80 V. The Nb 3d spectrum in Fig. 4 shows that only Nb₂O₅ 3d3/2 and Nb₂O₅ 3d5/2 peaks were observed on the outermost surface, and the ratio of constituent elements on the outermost surface of niobium oxide corresponds to Nb₂O₅. NbO was detected in the anodic layer when the sample was sputtered using an ion gun for 1 min and analyzed in the depth direction. Upon removing the topmost layer, the coating showed a mixture of Nb₂O₅ and NbO, with the ratio of NbO: Nb₂O₅ being around 6:4. After sputtering for 1 min, both samples prepared via anodizing Nb substrate at 60 and 80 V are seen in Figs. 7 and 8 demonstrate a transition from their topmost Nb₂O₅ layer to a mixture of Nb₂O₅ and NbO phases. Therefore, we conclude that the topmost Nb₂O₅ layer is independent of the applied voltage, while changes in color are observed as a result of different ratios of Nb₂O₅ and NbO phases deep inside the coating and depend on anodizing voltage, even when the surface layer exhibits same thickness.

Based on our analyses, the thickness of NbO-containing (mixed) layer was found to be linearly dependent on anodizing voltage applied, as well seen in Fig. 9.

Nb oxidation is known to proceed gradually through intermediate stages as follows: Nb → NbO and Nb₂O → Nb₂O₅. Ion sputtering (Figs. 7

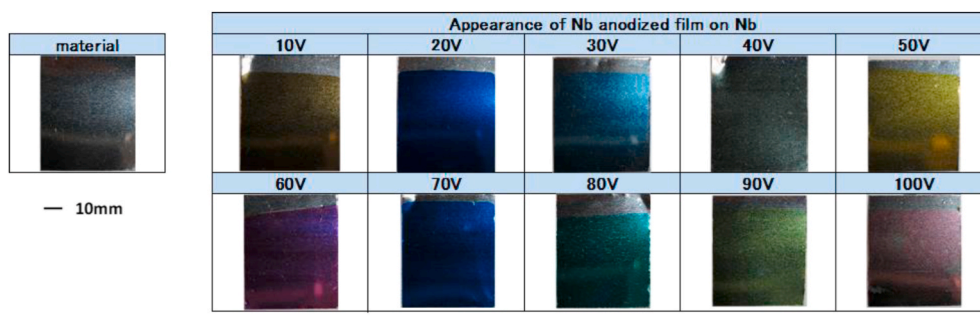


Fig. 3. Anodized layers prepared on Nb plates at different voltage.

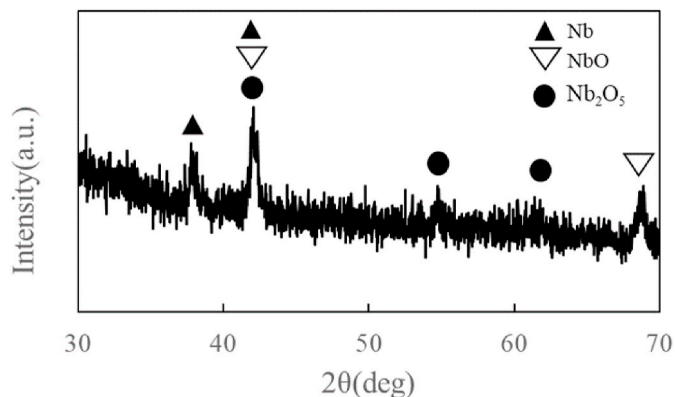


Fig. 4. XRD pattern of sample prepared via anodizing Nb substrate at 100 V.

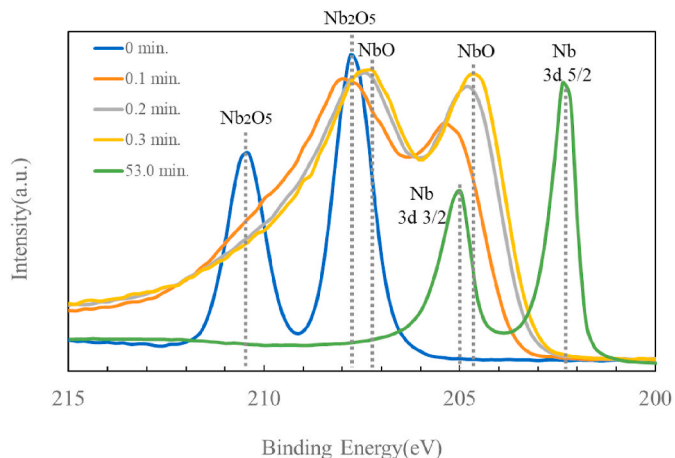


Fig. 5. XPS spectra of Nb 3d peaks prepared via anodization at applied voltage of 100 V. Lines with different colors correspond to topmost layer (blue) and layers after surface-sputtering for different times. (For interpretation of the references to color in this figure legend, the reader is referred to the Web version of this article.)

and 8) was performed every 0.1 min. The thickness of the anodized film formed at 20 V, 60 V, and 80 V was measured from the cross-sectional SEM, etched until the metal Nb appeared, and the time and film thickness were plotted to obtain the result, the detection depth was 0.4 nm/0.1 min. At the same time, Figs. 7–9 show that the anodizing voltage significantly affected the thickness of mixed NbO–Nb₂O₅ layer. As seen in Fig. 9, it was found to be 52.0, 108.0, and 160.0 nm for samples anodized at 20, 60, and 80 V, respectively. Thus, the topmost Nb₂O₅ layer was found to be less than 0.4 nm for all samples analyzed.

The obtained results agreed with the findings of Ono, which

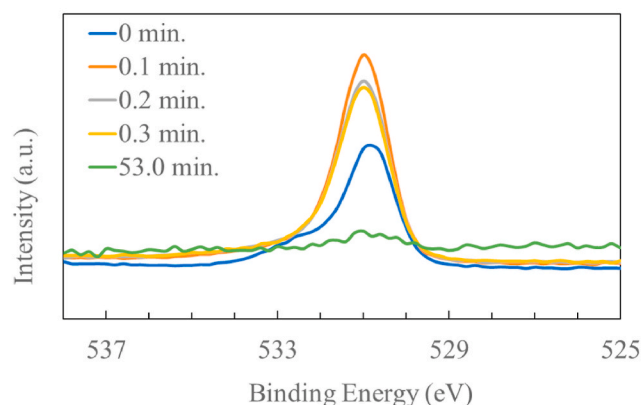


Fig. 6. XPS O1s spectra of sample prepared at applied voltage of 100 V. Lines with different colors correspond to topmost layer (blue) and layers after surface-sputtering for different times. (For interpretation of the references to color in this figure legend, the reader is referred to the Web version of this article.)

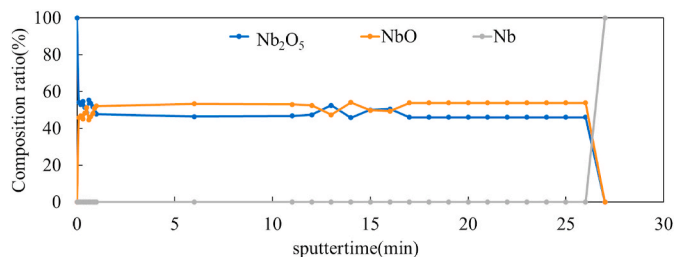


Fig. 7. Composition ratio of Nb₂O₅ prepared at applied voltage of 60 V.

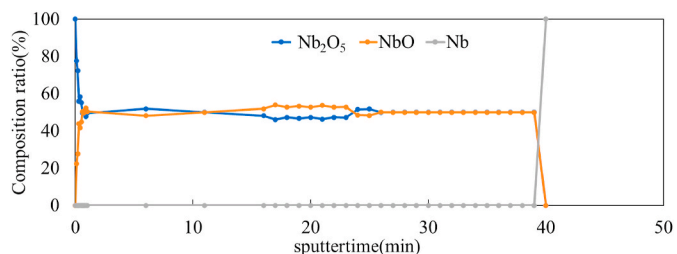


Fig. 8. Composition ratio of Nb₂O₅ prepared at applied voltage of 80 V.

depended on the electrolytic conditions [37]. The results show that the NbO film began to grow unstably during the initial stage of film growth irrespective of anodizing voltage applied, and such a mixed NbO–Nb₂O₅ layer grew linearly depending on the voltage value. Eventually, the

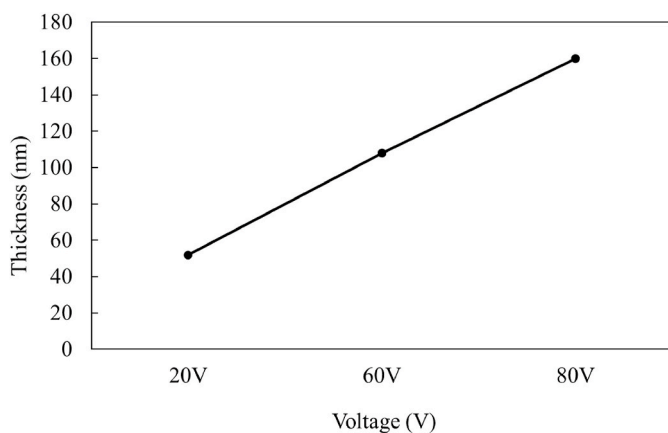


Fig. 9. Effect of anodizing voltage on thickness of NbO-containing mixed layer.

reactions stopped when the surface changed to Nb_2O_5 , and the growth stopped at the same time. Therefore, it can be concluded that the processing voltage led to a difference in the NbO film thickness, while the latter thickness affected the color of produced films. As reported by Ono, because the film thickness is independent of the film formation process, the thickness of the anodized film remains the same regardless of the applied voltage. According to the report of Tanaka [38], under a high electric field, the conduction in the anodized film is primarily ion conduction. Therefore, the thickness of the oxide layer increases with the electrolytic current; furthermore, the voltage applied to both ends of the film increases. It becomes extremely high and accounts for most of the bath voltage during alumite anodization. When the voltage reaches its saturation value, dielectric breakdown occurs. Simultaneously, the growth of conversion oxide layer stops, and the film formation reaches its limit [38]. Similar processes are expected in case of anodization on Nb surface. As shown above, the growth of NbO phase depends on the processing voltage. It is therefore believed that, similar to anodization of aluminum, oxidation reactions on niobium surface stop when dielectric breakdown occurs and the film formation reaches its limit. All the samples were found to have their topmost layer based on Nb_2O_5 phase with a thickness of below 0.4 nm, while the internal part of the formed layer was composed of NbO and Nb_2O_5 . Additionally, XPS results confirmed that the thickness of the part based on mixed NbO and Nb_2O_5 increased when higher values of applied voltage were used.

The electrical resistivity of NbO was $2 \times 10^{-7} \Omega\text{m}$, indicating that NbO is a conductive oxide. At the same time, the Nb_2O_5 phase is known as an insulating oxide, which is why when its pure layer formed on the outermost surface, the anodic oxidation reactions naturally stopped.

Next, we attempted to anodize the PI film, which is a flexible resin material. As the PI film is nonconductive, after surface modification using oxygen plasma treatment, a film of metal Nb was sputter-coated on its surface, after which the as-prepared structures were anodized. Finally, the colors of anodic films formed on both Nb and PI film substrates were optically compared.

3.2. Surface modification results

Fig. 10 shows how the wettability of PI film changes after its treatment with oxygen plasma. While the as-supplied PI film demonstrates the contact angle of water droplet of 61° (panel (A) in Fig. 10), after plasma treatment at 25 W for 1 min, the wettability was so high that the contact angle could not be measured (panel (B) in Fig. 10). This demonstrates that oxygen plasma treatment imparted good hydrophilicity to the PI surface.

Fig. 11 shows how the surface roughness of PI film changed as a result of oxygen plasma treatment under different conditions (plasma power and processing time). The surface roughness, evaluated with

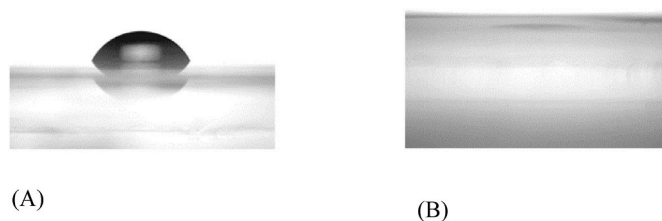


Fig. 10. Optical images of a water droplet on PI film: (A) before treatment (61°), and (B) after oxygen plasma treatment at 25 W for 1 min (0°).

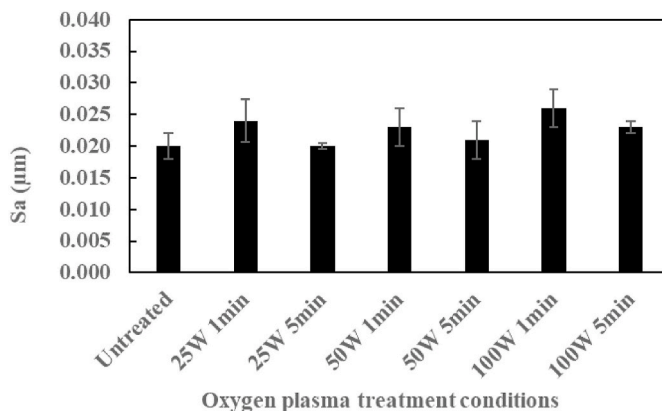


Fig. 11. Surface roughness of PI films treated with oxygen plasma.

white interference microscopy, is seen in Fig. 11 to be higher after the films were plasma treated. It was also found that longer processing with plasma led to somewhat smoother surfaces irrespective of plasma power used.

Next, XPS spectra of PI films subjected to plasma treatment were compared. In general, plasma-treated samples were found to exhibit a higher oxygen content than their as-supplied (untreated) counterpart, however, the O/C ratio observed in treated samples depended on plasma conditions (power and processing time). Fig. 12 shows the oxygen-to-carbon ratio of the samples after they were plasma treated, implying that more oxygen was incorporated into surface layer when higher-energy plasma was applied.

When PI films were treated at 100 W or higher, they were observed to get discolored. This was believed to be because of heat effect, indicating that the processing power was excessively high. The surface of such PI films plasma-treated at 100 W was found to be hydrophilized, become rougher, and enriched in oxygen (Fig. 12).

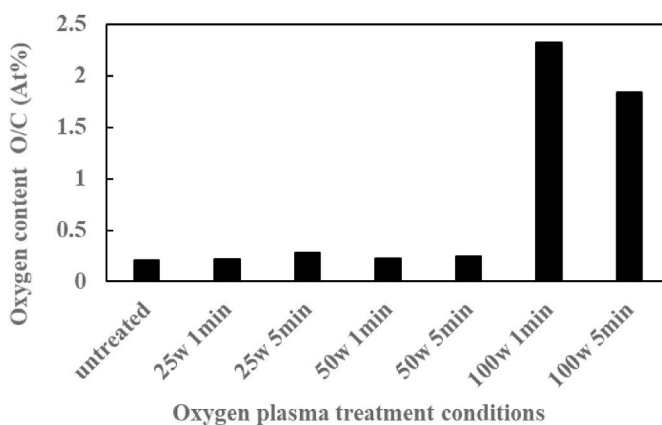


Fig. 12. Oxygen content in surface layer of PI films treated with oxygen plasma.

The effect of plasma treatment of PI substrates (power and time) on the adhesion strength of Nb film sputter-deposited on their surface was also evaluated, the results being exhibited in Fig. 13. The as-supplied untreated PI sample did not adhere to the metal film. The oxygen plasma treatment is seen in Fig. 13 to impart adhesion which was getting lower at higher treatment voltages [39].

Fig. 14 shows the XPS spectra (C 1s, O 1s) of a PI film in which the surface after the adhesive strength test was treated with 25 W (A, C, E) and 100 W (B, D, F) oxygen plasma for 1 min and N 1s peak).

Dotted line is the PI substrate, and solid line refers to (A, C, E) 25 W for 1 min and (B, D, F) 100 W for 1 min.

As seen in Fig. 14, plasma treatment at 25 W decreased the amount of surface N–C=O groups and increased that of C=O groups (531.0 eV). This can be attributed to increased oxygen content in the treated sample, which agrees well with its reduced water contact angle. Moreover, the increase in adhesion strength after the plasma treatment at 25 and 50/100 W occurred because the C=O peak providing the hydrophilicity increased based on the comparison between pristine and these plasma modified PIs. Furthermore, comparing the spectra of N 1s, it is considered that the adhesion was reduced because the C–N bond was reduced at 402.0 eV in the surface modification (F) at 100 W for 1 min. In the 100 W treatment, the surface modification effect was so strong that C–O–C bonds in the PI was broken, which suggests that the modified PI surface was unstable and weakened the adhesion. Especially, the 25 W treatment considerably increases. Moreover, a large difference can be observed in the C–O–C bond. At 25 W, the peak amount of C–O–C, which was the same as the material, however, it increased at 100 W owing to over oxidation of the PI. Furthermore, the distance between C–C and C–O–C is 1.5 eV, as reported in a previous study, and it is considered that identification is possible. This could be attributed to the debris of the material owing to the processing power, i.e., the close contact between the material and the Nb-sputtered film [30–33,40–43]. The surface was observed, and the difference in adhesion was evaluated. Although the surface roughness after the treatment did not significantly differ from that before the treatment, a detailed observation was performed using interference microscopy.

Fig. 15 shows no large difference was observed between PI film samples treated at 25 (B), 50 (C) and 100 W (D) for 1 min. However, under higher magnification, the surface treated at 100 W was found to have more nano-scaled rough features in comparison with its counterpart plasma-processed at 25 W. This agrees well with the above mentioned conclusions drawn from XPS results on higher damage to the film caused by high-power plasma.

Furthermore, atomic force microscopy (AFM) was also applied to compare PI surface both before and after processing with oxygen plasma, with Fig. 16 showing surface images of as-supplied (A) and treated at 25 W for 1 min (B) samples. The untreated material is seen to

have a smooth AFM image, while upon plasma treatment nano-scaled roughness was created (panel (B)). The latter roughness is believed to result in improvement of adhesion when metal Nb film was then sputter-deposited on the plasma-treated PI substrate.

Altogether, the above observations suggested us to choose plasma treatment of PI films at 25 W for 1 min, which provides the best adhesion of sputter-coated metal Nb film that can survive anodizing successfully. Thus, metal Nb films were deposited on such plasma-pretreated PI films, which upon anodizing under different conditions gave rise to various rich colors, similar to those produced via anodizing Nb plates. Fig. 17 presents optical images of anodic Nb films produced at different voltage on PI film substrates. It is clearly seen that anodic films with a wide range of colors could be fabricated.

The AFM observation of the anodized films on PI substrates was also performed. Panels (A) and (B) in Fig. 18 compare two films anodized at 20 V and 100 V, respectively. The film treated at 20 V, where a thin anodic layer of Nb oxides formed (Fig. 18 (A)), shows nano-sized irregularities, basically repeating the relief demonstrated by its plasma-treated PI substrate. Its much thicker anodic counterpart formed at 100 V looks much smoother (see panel (B) in Fig. 18), from which one can assume that the thicker film filled the irregularities on its PI substrate.

Fig. 19 shows XPS Nb 3d spectra of the samples produced via anodizing Nb on PI (orange) and Nb (blue) substrates, both samples prepared at 100 V. The maximum peak corresponding to Nb₂O₅ bonding is seen at approximately 207.2–207.8 eV for both samples, their spectral having basically identical shapes in Fig. 19. This implies that the outermost surface of both samples was composed of Nb₂O₅, as both spectra are consistent with previously reported data for Nb₂O₅ [44].

Fig. 20 shows reflectance spectra of anodic films produced on Nb substrates at anodizing voltage of 20, 60, and 100 V, while similar data for similar samples prepared on PI substrates are presented in Fig. 21. For comparison, non-anodized Nb surfaces on the same substrates are also presented in Figs. 20 and 21 (marked as 0 V). It is seen in Figs. 20 and 21 that the prepared anodic films were 20–30% less reflective than their non-anodized counterparts (a metal Nb sputter-deposited film on PI film, and a Nb substrate itself). The Nb films sputtered onto PI film were as thin as 500 nm. After anodization, their reflectance spectra exhibited similar trends.

Finally, as demonstration of very good adhesion, Fig. 22 shows an anodized Nb sample deposited on PI film as the whole system is mechanically bent. It is thus visually confirmed that the metallic film is very well adhered to its PI substrate and they both survive the bending test. Keeping in mind that the color of such anodic Nb oxide films can be controlled within a wide range of shades, the technology proposed in this study on preparing thin anodic Nb films on flexible PI substrates looks promising and can find its applications.

4. Conclusions

This study is focused on how anodic films grow on the surface of both bulk Nb and thin metal film of Nb pre-deposited onto polyimide (PI) films as substrates. At first, we show that the overall thickness of anodic oxide films on Nb is proportional to anodizing voltage, with the topmost layer always being Nb₂O₅ phase and below ~0.4 nm in thickness, and the deeper part being a mixture of NbO and Nb₂O₅ phases irrespective of voltage applied.

Then, we deposit a thin layer of Nb (~500 nm) onto commercially available PI films and show that when anodized, this two-layered structure demonstrates anodic oxide films with the same characteristics (thickness and phase composition) as those produced on bulk metal Nb. To impart good adhesion of metal Nb films sputter-deposited on PI substrates, the latter substrates were pre-treated with oxygen plasma. When sputter-coated under optimal conditions, such Nb films survived the bending test even after anodization during which Nb oxide films with a variety of colors was formed.

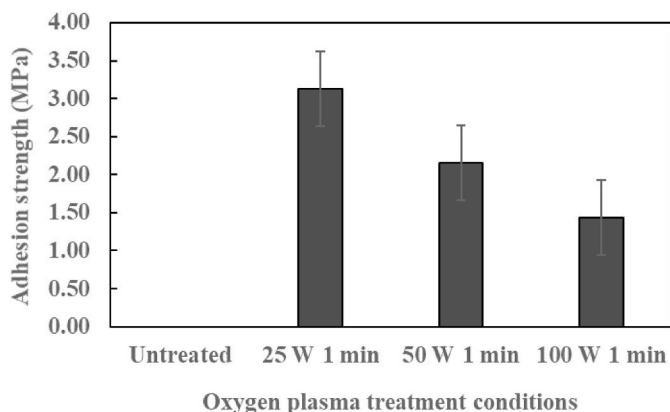


Fig. 13. Adhesion strength of Nb films sputter-deposited on plasma-treated PI substrates.

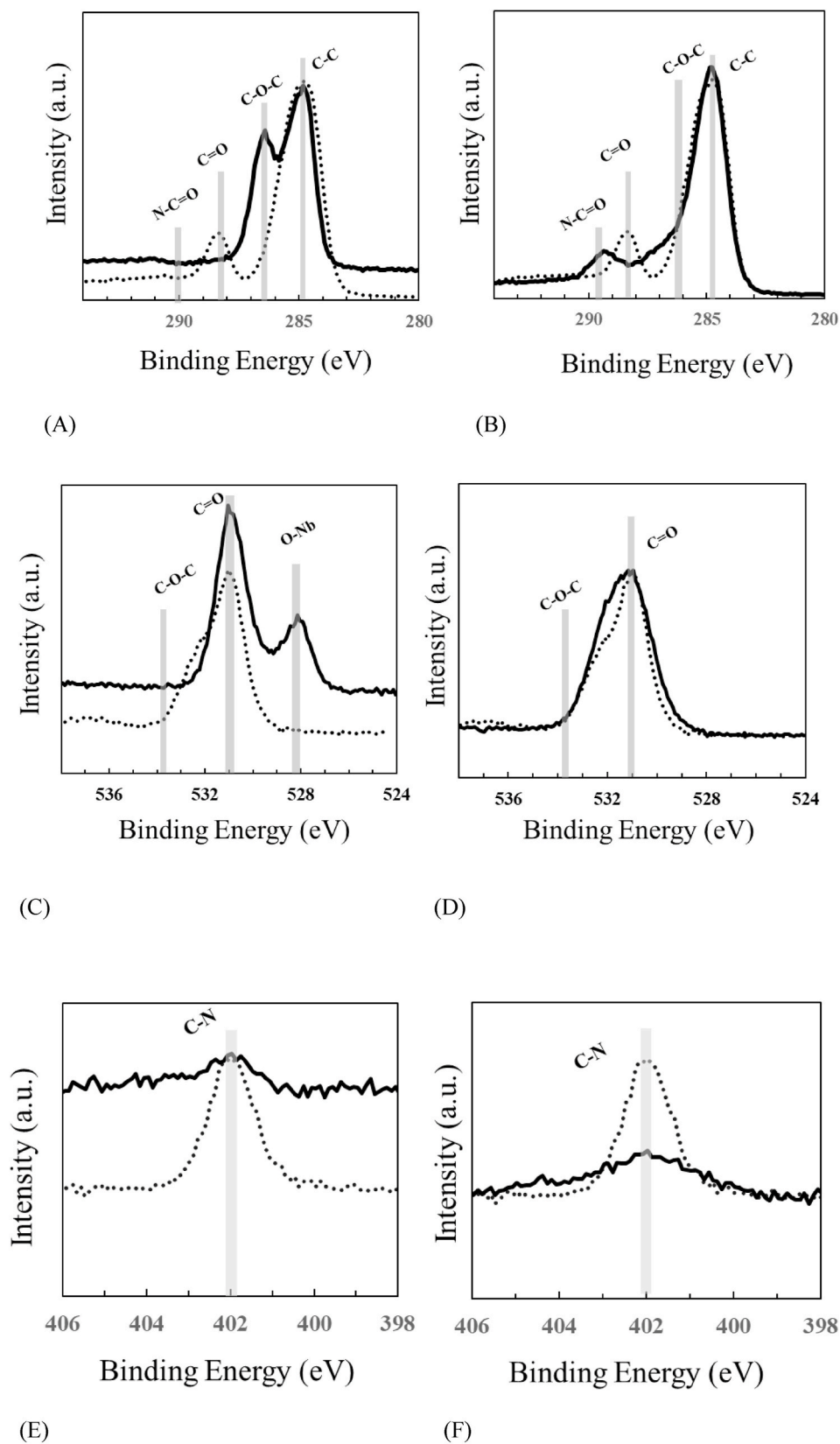


Fig. 14. XPS spectra of PI films after theadhesion strength test. (A) and (B) C 1s spectra, (C) and (D) O 1s spectra, and (E) and (F) N 1s spectra.

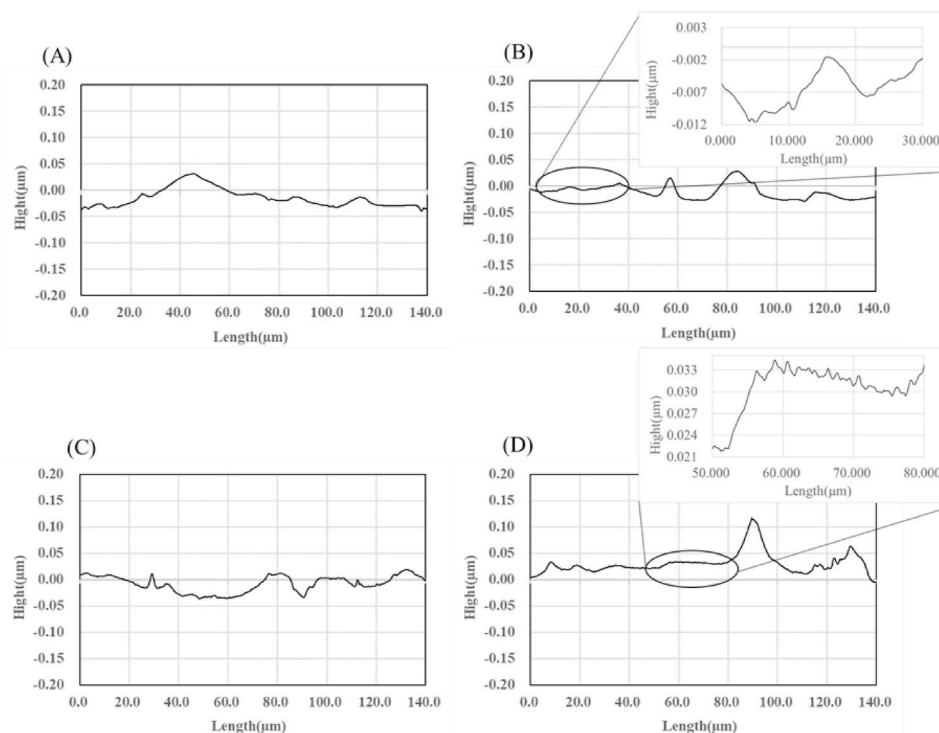


Fig. 15. Microscopic observation of PI samples treated with oxygen plasma: (A) untreated PI film, (B) PI surface treated at 25 W for 1 min, (C) surface treated at 50 W for 1 min, and (D) PI surface treated at 100 W for 1 min.

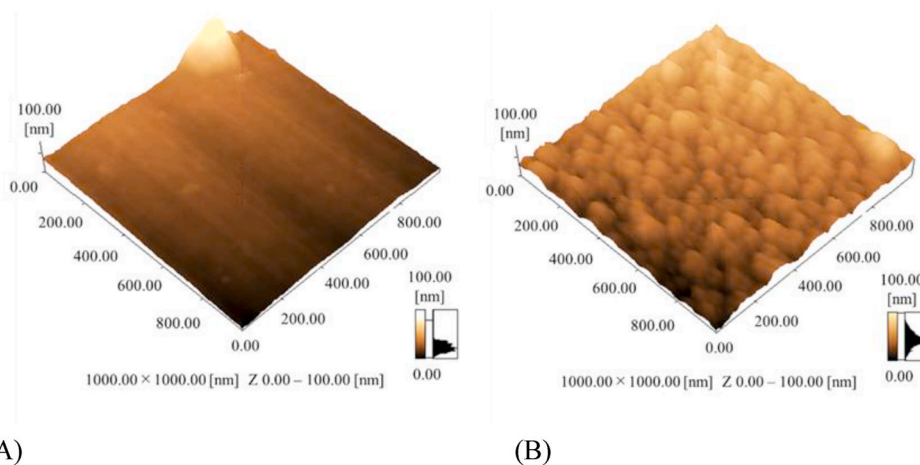


Fig. 16. AFM surface images of non-modified PI surface. (A) and PI surface treated by plasma at 25 W for 1 min (B).

Nb sputtered film on PI film	Appearance of Nb anodized film on PI				
	10V	20V	30V	40V	50V
					
	60V	70V	80V	90V	100V
					

Fig. 17. Optical images of anodic Nb films produced at different anodizing voltages on PI film substrates.

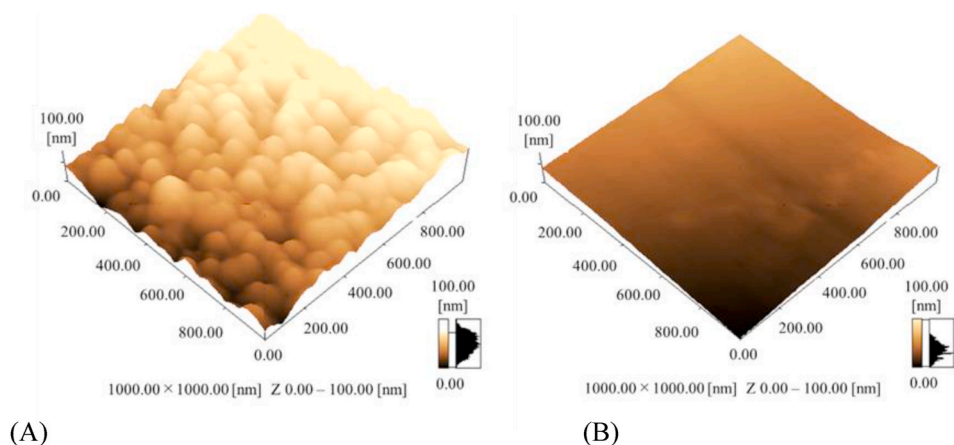


Fig. 18. AFM surface images of samples prepared at anodization voltage of 20 V (A) and 100 V (B).

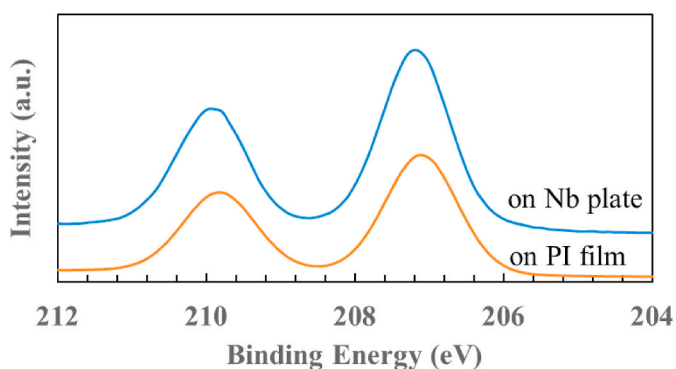


Fig. 19. XPS Nb 3d spectra of anodized Nb films formed on PI (orange spectrum) and Nb substrate (blue spectrum). (For interpretation of the references to color in this figure legend, the reader is referred to the Web version of this article.)

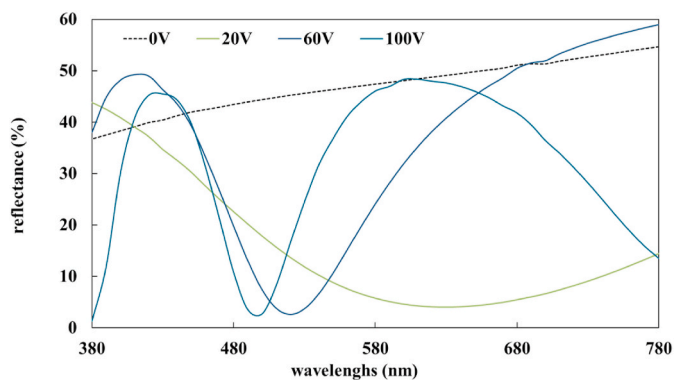


Fig. 20. Reflectance of anodic films prepared on Nb substrates at different anodization voltages.

Thus, this work demonstrates a new technology to prepare anodic Nb oxide films on commercial PI films. The good adhesion between anodic Nb oxide layer and its flexible PI substrate, as well as a wide variety of colors provided by anodic films produced at different anodizing voltages, allow us to expect that this promising technology can find industrial applications.

Declaration of competing interest

The authors declare that they have no known competing financial

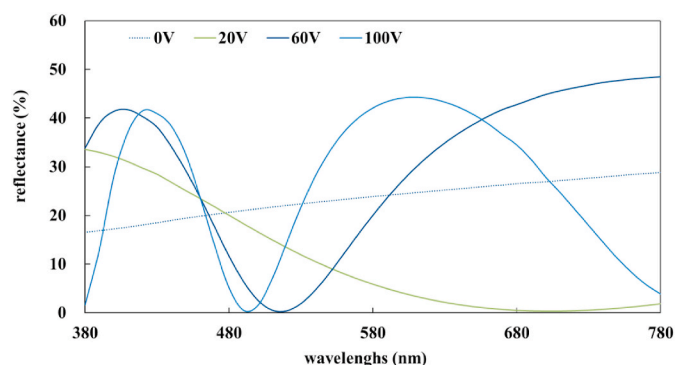


Fig. 21. Reflectance of anodic films prepared on PI substrates at different anodization voltages.

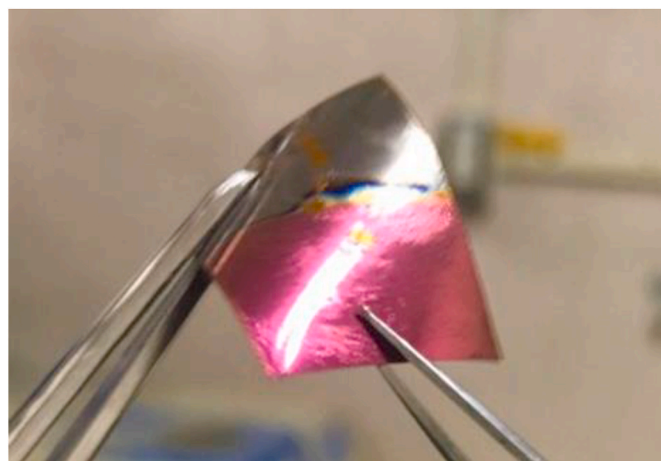


Fig. 22. Bending test of anodic Nb oxide film on PI film as substrate.

interests or personal relationships that could have appeared to influence the work reported in this paper.

Acknowledgments

The authors would like to thank Enago (www.enago.jp) for the English review. The authors would also like to thank Mr. Masaki Morikawa associated with the Advanced Physical Properties Evaluation Office for his guidance in the XPS analysis in Advanced Analysis Centre of Research Institute of Science and Technology of Tokai University.

References

- [1] R.J. Holmberg, D. Beauchemin, G. Jerkiewicz, Characteristics of colored passive layers on titanium: morphology, optical properties, and corrosion resistance, *ACS Appl. Mater. Interfaces* 6 (2014) 21576–21584.
- [2] D. Gallant, M. Pezolet, S. Simard, Optical and physical properties of cobalt oxide films electrogenerated in bicarbonate aqueous media, *J. Phys. Chem. B* 110 (2006) 6871–6880.
- [3] G. Jerkiewicz, B. Zhao, S. Hrapovic, B.L. Luan, Discovery of reversible switching of coloration of passive layers on titanium, *Chem. Mater.* 20 (2008) 1877–1880.
- [4] S.N. Wosu, Anodic oxidation of tantalum in water and biological solutions using current limiting constant voltage method, *J. Mater. Sci.* 42 (2007) 4087–4097.
- [5] C.C. Sheng, Y.Y. Cai, E.M. Dai, C.H. Liang, Tunable structural color of anodic tantalum oxide films, *Chin. Phys. B* 21 (2012). <http://www.ncbi.nlm.nih.gov/pubmed/088101>.
- [6] I. Komatsu, H. Aoki, Y. Ito, S. Maeda, Niobium films as rewritable imaging media, *Nihon Gazo Gakkaishi* 55 (2016) 22–26 ([in Japanese]).
- [7] K. Kuroda, *World of Interference Color, Art and Technology, Titanium and Niobium*, Koshinsha, 2007 [in Japanese].
- [8] I. Mjeiri, R. Groccassan, A. Rougier, Enhanced coloration for hybrid niobium-based electrochromic devices, *ACS Appl. Energy Mater.* 1 (2018) 4359–4366.
- [9] F. Kang, H. Zhang, L. Wondraczek, Xiaobao Yang, Y. Zhang, D.Y. Lei, B.-G. Mingying Peng, Modulation in single Bi³⁺-Doped yttrium–scandium–niobium vanadates for color tuning over the whole visible spectrum, *Chem. Mater.* 28 (2016) 2692–2703.
- [10] J. He, L. You, D.T. Tran, J. Mei, Low-temperature thermally annealed niobium oxide thin films as a minimally color changing ion storage layer in solution-processed polymer electrochromic devices, *ACS Appl. Mater. Interfaces* 11 (2019) 4169–4177.
- [11] J. Edlinger, J. Ramm, H.K. Pulker, Properties of ion-plated Nb₂O₅ films, *Thin Solid Films* 175 (1989) 207–212.
- [12] F. Lai, L. Lin, Z. Huang, R. Gai, Y. Qu, Effect of thickness on the structure, morphology and optical properties of sputter deposited Nb₂O₅ films, *Appl. Surf. Sci.* 253 (2006) 1801–1805.
- [13] J.-P. Masse, H. Szymanski, O. Zabeida, A. Amassian, J.E. Klemberg-Sapieha, L. Martinu, Stability and effect of annealing on the optical properties of plasma-deposited Ta₂O₅ and Nb₂O₅ films, *Thin Solid Films* 515 (2006) 1674–1682.
- [14] S. Venkataraj, R. Drese, Ch Liesch, O. Kappertz, R. Jayavel, M. Wuttig, Temperature stability of sputtered niobium–oxide films, *J. Appl. Phys.* 91 (2002) 4863–4871.
- [15] S.A. O'Neill, I.P. Parkin, R.J.H. Clark, A. Mills, N. Elliott, Atmospheric pressure chemical vapour deposition of thin films of Nb₂O₅ on glass, *J. Mater. Chem.* 13 (2003) 2952–2956.
- [16] T. Maruyama, S. Arai, Electrochromic properties of niobium oxide thin films prepared by radio-frequency magnetron sputtering method, *Appl. Phys. Lett.* 63 (1993) 869–870.
- [17] G. Ramírez, S.E. Rodil, S. Muhl, D. Turcio-Ortega, J.J. Olaya, M. Rivera, E. Camps, L. Escobar-Alarcón, Amorphous niobium oxide thin films, *J. Non-Cryst. Solids* 356 (2010) 2714–2721.
- [18] Viswanathan S. Saji, Superhydrophobic surfaces and coatings by electrochemical anodic oxidation and plasma electrolytic oxidation, *Adv. Colloid Interface Sci.* 283 (2020) 102245.
- [19] J. Edlinger, J. Ramm, H.K. Pulker, Properties of ion-plated Nb₂O₅ films, *Thin Solid Films* 175 (1989) 207–212.
- [20] I. Komatsu, H. Aoki, M. Ebisawa, A. Kuroda, K. Kuroda, S. Maeda, Color change mechanism of niobium oxide thin film with incidental light angle and applied voltage, *Thin Solid Films* 603 (2016) 180–186.
- [21] M. Ohring, *The Materials Science of Thin Films, Engineering, Materials Science Academic Press*, 1995, pp. 18–21.
- [22] Q.-D. Ling, D.-J. Liaw, C. Zhu, D.S. Chan, E. Kang, K. Neoh, Polymer electronic memories: materials, devices and mechanisms, *Prog. Polym. Sci.* 33 (2008) 917–978.
- [23] J. Chen, Raul D. Rodriguez, E. Sheremet, Y. Wang, E. Sowade, R.R. Baumann, Z. Feng, Surface modification with special morphology for the metallization of polyimide film, *Appl. Surf. Sci.* 487 (1) (2019) 503–509.
- [24] I.-H. Tseng, T.-Ta Hsieh, C.-H. Lin, M.-H. Tsai, D.-L. Ma, C.-J. Kod, Phosphinated polyimide hybrid films with reduced melt-flow and enhanced adhesion for flexible copper clad laminates, *Prog. Org. Coating* 124 (2018) 92–98.
- [25] K. Miyauchi, M. Yuasa, A study of adhesive improvement of a Cr-Ni alloy layer on a polyimide surface by low pressure gas plasma modification, *Prog. Org. Coating* 76 (2013) 1536–1542.
- [26] E. Cunaj, P.S. Petrou, G.D. Kaprou, S.E. Kakabakos, E. Gogolides, A. Tserepi, Oxidation behavior of the B-modified silicide coating on Nb-Si based alloy at intermediate temperatures, *Surf. Coating Technol.* 334 (2018) 292–299.
- [27] Y. Oh, E.J. Kim, Y. Kim, K. Choi, W.B. Han, H.-S. Kim, C.S. Yoon, Adhesion of sputter-deposited Cu/Ti film on plasma-treated polymer substrate, *Thin Solid Films* 600 (2016) 90–97.
- [28] T. Yonemoto, J. Sato, H. Nemoto, M. Mita, Adhesion of sputtered Cu films on polyimide films exposed with various ion species, *Shinku* 36 (1993) 337–339 ([in Japanese]).
- [29] K.N. Kim, S.M. Lee, A. Mishra, G.Y. Yeoma, Atmospheric pressure plasmas for surface modification of flexible and printed electronic devices: a review, *Thin Solid Films* 598 (2016) 315–334.
- [30] G. Greczynski, L. Hultman, X-ray photoelectron spectroscopy: towards reliable binding energy referencing, *Prog. Mater. Sci.* 107 (2020) 100591.
- [31] G. Greczynski, L. Hultman, C 1s peak of adventitious carbon aligns to the vacuum level: dire consequences for material's bonding assignment by photoelectron spectroscopy, *ChemPhysChem* 18 (2017) 1507.
- [32] G. Greczynski, L. Hultman, Compromising science by ignorant instrument calibration—need to revisit half a century of published XPS data, *Angew. Chem. Int. Ed.* 59 (2020) 5002.
- [33] G. Greczynski, L. Hultman, Reliable determination of chemical state in x-ray photoelectron spectroscopy based on sample-work-function referencing to adventitious carbon: resolving the myth of apparent constant binding energy of the C 1s peak, *Appl. Surf. Sci.* 451 (2018) 99.
- [34] S. Iwamori, N. Yanagawa, M. Sadamoto, R. Nara, S. Nakahara, Polyimides and Other High Temperature Polymers 2 (2003) 407–418.
- [35] G.E. McGuire, G.K. Schweitzer, Thomas A. Carlson, Core electron binding energies in some Group IIIA, VB, and VIB compounds, *Inorg. Chem.* 12 (1973) 2451.
- [36] R. Fontaine, R. Caillat, L. Feve, M.J. Guittet, Déplacement Chimique esca dans la serie des oxydes du niobium, *J. Electron. Spectrosc. Relat. Phenom.* 10 (1977) 349–357.
- [37] S. Ono, Formation behavior and control factors of anodic films on niobium, *J. Surf. Finish. Soc. Jpn.* 54 (2003) 447–451 ([in Japanese]).
- [38] Y. Tanaka, Voltage and current control in anodic oxidation, *J. Surf. Finish. Soc. Jpn.* 68 (2017) 260–269 ([in Japanese]).
- [39] Q. Ma, W. Zhao, Xirong Li, L. Li, Z. Wang, Study of an environment-friendly surface pretreatment of ABS-polycarbonate surface for adhesion improvement, *Int. J. Adhesion Adhes.* 44 (2013) 243–249.
- [40] T. Kondo, R. Watanabe, Y. Shimoyama, K. Shinohe, S.A. Kulinich, S. Iwamori, Effect of reactive oxygen species generated with ultraviolet lamp and plasma on polyimide surface modification, *Surf. Interface Anal.* 49 (2017) 1069–1077.
- [41] F. Lin, W. Li, Y. Tang, H. Shao, C. Su, J. Jiang, N. Chen, High-performance polyimide filaments and composites improved by O₂ plasma treatment, *Polymers* 10 (2018) 695, <https://doi.org/10.3390/polym10070695>.
- [42] D. Wolany, T. Fladung, L. Duda, J.W. Lee, T. Gantenfort, L. Wiedmann, A. Benninghoven, Combined ToF-SIMS/XPS study of plasma modification and metallization of polyimide, *Surf. Interface Anal.* 27 (1999) 609–617.
- [43] N. Inagaki, S. Tasaka, H. Ohmori, S. Mibu, Improvement in the adhesion between copper metal and polyimide substrate by plasma polymer deposition of cyano compounds onto polyimide, *J. Adhes. Sci. Technol.* 10 (1996) 243–256.
- [44] P.C. Karulkar, Effects of sputtering on the surface composition of niobium oxides, *J. Vac. Sci. Technol.* 18 (1981) 169–174.